

Durability & Microstructure Studies of Fly ash based Geopolymer Mortar.Bohra Vinay Kumar Jain^{1*}, Nerella Ruben², Madduru Sri Rama Chand³^{1*}Research Scholar, Dept. of Civil Engg. Vignana's Foundation for Science Technology & Research University, Vadlamudi, Guntur, 522213, India, bohravinay.vinay@gmail.com²Assoc. Prof., Dept. of Civil Engg. Vignana's Foundation for Science Technology & Research University, Vadlamudi, Guntur, 522213, India, rubennerella2512@gmail.com.³Asst. Prof., Dept. of Civil Engg., Sree Chaitanya College of Engineering, Karimnagar, Telangana, 505527, India, maddurusriram@gmail.com**Abstract:**

This article discusses the microstructure, strength, and durability of geopolymer mortar constructed using low calcium fly ash (Class -F). Geopolymer mortars are made by combining fly ash and sand with an alkaline solution (Sodium hydroxide (NH) and sodium silicate (NS)). The ratio of fly ash to sand is 1 to 1, with a constant rate of alkaline liquid to fly ash of 0.55 and NS/NH ratios of 1.5, 2, 2.5, 3, respectively. The geopolymer mortars for the ambient and oven-cured samples were made by varying the NH concentrations to 2, 4, 6, and 8M. The curing temperature of 60°C for twenty-four hours kept the geopolymerization active. The results indicated that the thick polymerisation gel development in the SEM pictures and XRD analysis explains the presence of the mineral Microcline and sodium-calcium silicate and is consistent with the findings of the EDS analysis. The SEM photos reveal the production of a robust polymerisation gel. The XRD data quantified the percentage of minerals created, making the material suitable for construction to fulfil present and future needs.

Keywords: durability properties, Microstructure analysis, XRD, SEM

Introduction:

Ashes from fly ash are increasingly becoming a primary material in the construction industry. As a by-product of the process, it is created in coal combustion units, most of which are located in thermal power stations. In general, coal is a heterogeneous mixture of components. The combustion of bituminous and sub-bituminous coal in power plants that are burnt to temperatures between 1400 and 1600 degrees Celsius creates class F, and Class C fly ashes from silos. Fly ash can be divided into class C (sub-bituminous) and F (bituminous). Both of these categories are used extensively. According to ASTM C 618, it is abundantly evident that the fly ash in question is class F if the percentages of silica, alumina and iron oxide in it are greater than or equal to 70%. Fly ash classified as class C comprises at least 50 per cent of the total. These days, building businesses and other industries are looking for an alternative to cement, which is why many studies are going on into geopolymer binders and their future applications. The alkaline solution and the source materials are the two most essential components in fabricating geopolymer binders. Reference materials should have a high concentration of silica and aluminium, which can be obtained from a wide variety of source materials, including rice husk ash, wasted coffee, GGBS, clays, fly ash, metakaolin, and perlite. The solution is produced by pellets containing either potassium or sodium (based on the concentration). The use of fly ash in the geopolymer production process can lead to a reduction in greenhouse gas emissions and the production of environmentally friendly and responsible materials [1-4,7,10-11,13-15]. Creating a three-dimensional network can be attributed to mixing geopolymer solutions with source materials [8]. The geopolymer may also benefit structural health monitoring structures, mainly decaying structures, if used adhesives based on metakaolin. [2] This may be possible if the geopolymer is used. Geopolymers based on fly ash and slag can effectively stabilise soil [16-17]. In addition, the geopolymer binders exhibit outstanding qualities, such as early compressive strength, minimal creep and shrinkage, and resilience even to attacks on durability [5-7,12]. The fineness of the fly ash used in the construction determines the outstanding properties exhibited. The author separated the fly ash from the Mae Moh power station into coarser, medium, and more refined types of fly ash for the study. He found that fine fly ash has a very high compressive strength compared to the other two types of fly ash, and he used high calcium fly ash for his experiments [3]. Bottom ash has also demonstrated excellent qualities when high calcium fly ash is used in geopolymer mortars of mean diameters 15, 25, and 32 m, respectively [4]. These geopolymer mortars have also shown that bottom ash may achieve these remarkable properties. Compared to OPC, not only is it possible to improve strength with GPC, but its endurance also increases thanks to increased resistance to chloride attack [6]. Compared to OPC, both types of fly ashes are subjected to the influence of the alkali-silica reaction, which may be investigated through the microstructural investigation with techniques such as SEM,

XRD, FTIR, and compressive strength [5]. The crack formation may be spotted using a scanning electron microscope for geopolymer samples. Mineral components can be identified using an X-ray diffractometer, and the author stated that albite is responsible for the strength augmentation of GPC specimens. FTIR was utilised to investigate the bond formation of GPC, and the ASR reaction was carried out in GPC [5]. EDS and TG/DTA can be used to determine the elemental composition of geopolymers, and these materials can withstand high temperatures without changing their properties. The primary objective of this research is to investigate and evaluate the material's resistance to degradation when subjected to sulphuric acid at a concentration of 5%, followed by XRD and SEM microstructural examination. This document presents the results based on the tests and analyses conducted using various methods.

Experimental details:

Materials:

The Vijayawada thermal power plant in Andhra Pradesh, India, provided the low calcium fly ash used in this process. Scanning electron microscopy (SEM) reveals that the fly ash is predominantly spherical [3], and the energy dispersive spectroscopy (EDS) analysis shows that the primary chemical components of the fly ash are 38.6% SiO₂, 18.5% Al₂O₃, 14.7% Fe₂O₃, and 12.4% CaO. Fly ash particles have a specific gravity of 2.21 and a Blaine fineness of 4050 cm²/g. The mean diameter of fly ash particles is 10-25 μm. The sodium silicate (Na₂SiO₃) pellets with 18.32% Na₂O, 30.76% SiO₂, and 50.82% H₂O and the sodium hydroxide (NaOH) pellets with 98% purity are the alkali activators that are utilised in this setting. For the production of geopolymer mortar, the fineness modulus of the sand used was 2.39, and the specific gravity of the sand was 2.62. The sand was sourced locally from the ocean and is typically located in Zone – II.

Mix proportions, mixing, and casting:

In this instance, the ratio of fly ash to sand was maintained at 1:1. The NS/NH values were varied as follows: 1.5, 2, 2.5, 3, and an alkaline liquid-to-binder ratio of 0.55 was utilised for the mixing of geopolymer mortars. The influence of several concentrations of sodium hydroxide on geopolymer mortars, specifically 2, 4, 6, and 8 Molar, is investigated in this study. The concentrations are as follows: (M). To ensure that the particles are well dissolved, mixing the geopolymer components takes place in a Hobart mixer for a few minutes (approximately up to 3-5 minutes). After that, the combined elements are compressed using a vibrating machine on mortar cubes of 70.7 millimetres on one side, 70.7 millimetres on the length, and 70.7 millimetres on the height. The specimens were preserved in wet and dry curing conditions (i.e., Ambient and oven cured). The samples were held in the range for 24 hours at a temperature of 60 degrees Celsius, and the ambient temperature was maintained at a controlled 27 degrees Celsius until they were examined.

Testing details:

Compressive strength test:

Mortar cubes of varying ages are tested using a digital machine, and the results are recorded using a pacing value of 1.2KN/sec by IS 516-1956 [19]. CTM's capacity is 100T, and the readings are recorded using this pacing value.

Durability tests:

1) Acid attack test:

The acid attack test was conducted for the geopolymer mortar specimens at different ages of the models. The chemical resistance of the geopolymer mortar sample was prepared for different molarities and ratios and understanding its behaviour in both the 5% sulphuric acid. This test was carried out by ASTM C 666-1997. The acid mass loss factor (AMLF) measures the amount by which the mass of the specimen has changed; the acid attack factor (AAF) measures the amount by which the dimensions have changed, the acid strength loss factor (ASLF), which measures the amount by which the strength of the samples has changed, and the acid durability loss factor (ADLF), which combines all of the mass, dimension, and strength of the models, determines the final value for the samples after 7, 14, 28, 56, and 90 days of immersion. We measured its mass, dimension, and strength and computed the acid durability loss factor.

XRD: The measurements of phase identification, percentage of crystallinity, and molecular structure can all be accomplished using X-ray diffraction. The Rigaku micro flex 600, manufactured in Japan by the Rigaku corporation and representing the 6th generation of that company's design, is the instrument we are employing. The voltage range for the device must be between 100 and 240 volts, and the frequency must be between 50 and 60 hertz. The basic unit of the instrument has a mass of around 80 kilogrammes, and the technology utilised is a tabletop x-ray diffractometer equipped with a sophisticated detector. The ability of this instrument to do a phase analysis of polycrystalline materials is the primary advantage of employing it. It is possible to record it on the computer of the external PC, which should preferably use an operating system based on Microsoft Windows and PDXL Software.

SEM: The scanning electron microscope is a VEGA SB model with settings for a high-vacuum, three-axis motorised SEM system, and its configuration parameters read as follows: The SB chamber is suspended mechanically and has ten ports, a door that is 120mm wide, and an interior diameter of 160mm. Additionally, the chamber's internal size measures 160mm in diameter. The software included with the instrument assists with the analysis of picture processing, as well as an object's area, hardness, and multiple image calibrations. The instrument's accelerating voltage can range from 200V to 30kV, its scanning speed can be varied in stages or continuously from 20ns to 10ms per pixel, and its resolution can be as high as 3nm at 30keV for the high vacuum mode SE and as low as 3.5nm at 30keV for the low vacuum mode BSE. The instrument's user-friendliness and availability in multiple languages, its simple control of SEM for even inexperienced users, its assistance in image management and report creation, and its speedy access to routine investigations are some of the reasons why its utilisation is so important.

Test Results and discussion:

Durability:

Acid Mass Loss Factor:

The acid mass loss factor is the change in the mass of the sample after immersion in the 5% sulphuric acid. Its original group of the sample constitutes its Acid Mass Loss Factor (AMLF), and it can write as

$$(AMLF)_{\text{DAYS}} = \frac{(\text{mass change in the sample after immersion in sulphuric acid})}{(\text{mass of the sample before immersion in sulphuric acid})} \times 100$$

The fig:1 shows the AMLF for 2M, 4M, 6M and 8M for the alkaline ratio of NS/NH= 1.5, 2, 2.5 and 3 for 7, 14, 28, 56 and 90 days, respectively. Here if the samples were placed in 5% sulphuric acid and its mass loss was observed at all ages. For 2M, we see its mass loss was as high as 10%, 4M, the mass loss was as high as 8%, 6M was 9%, and 8M was 8%. But if we look into the ratio of alkaline ratios of 1.5, 2, 2.5, and 3, then we get a clear overview of the mass loss for all the ages; the lesser is the mass loss for a ratio of 2.5 for all the other ratios.



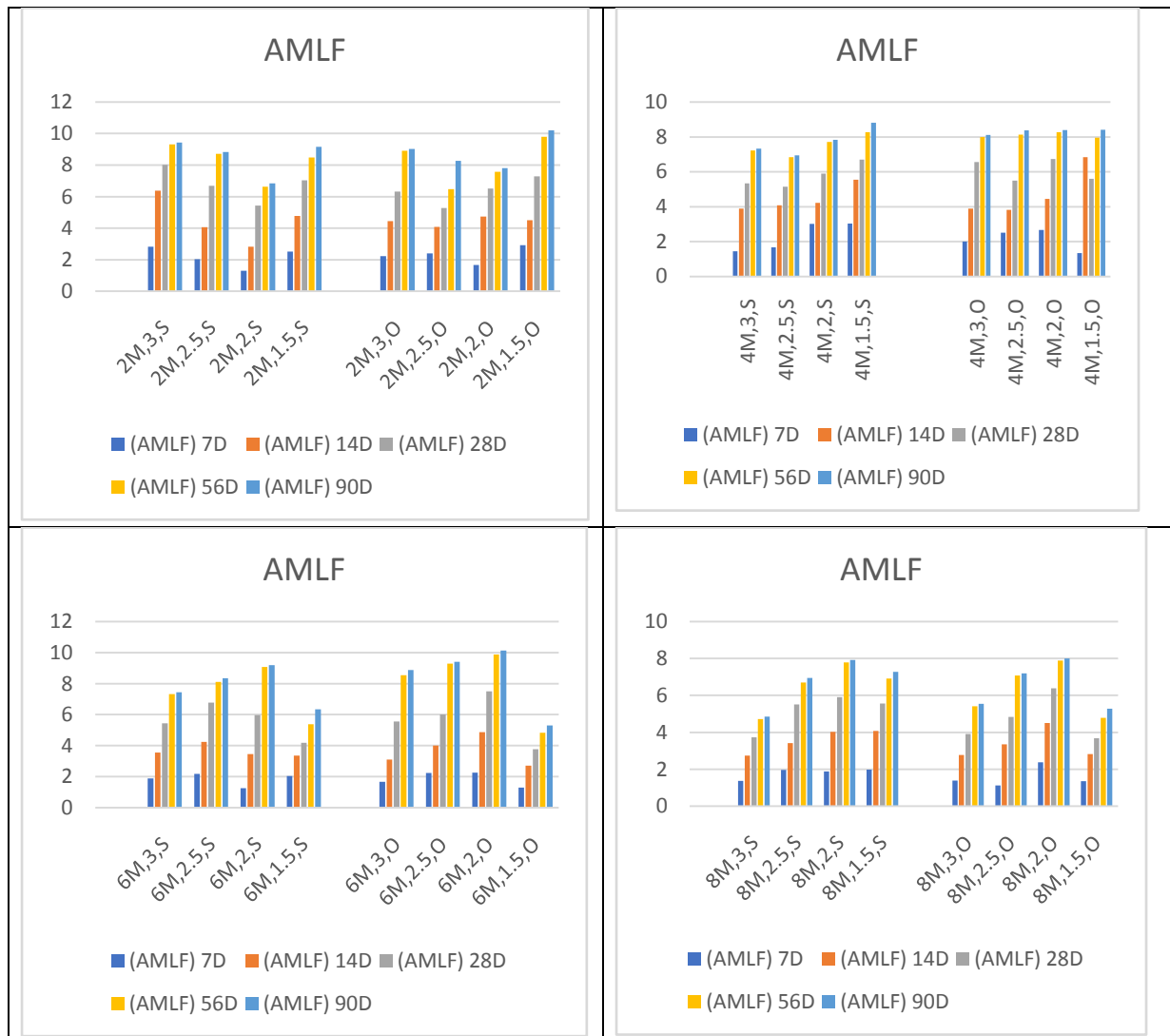


Fig: 1: AMLF of Geopolymer Mortars 2,4,6,8M & NS/NH=1.5,2,2.5,3 for 7,14,28,56,90Days in Ambient(S) & Oven(O) in H_2SO_4

Acid Attack Factor: the acid attack factor can be defined as the change in the dimensions along its diagonal of the specimen after immersion in the sulphuric acid to the original dimensions of the sample before immersion it can write as

$$(AAF)_{DAYS} = \frac{(\text{change in the sample dimension after immersion in sulphuric acid})}{(\text{original dimension of the sample before immersion in sulphuric acid})} \times 100$$

Fig:2 shows the acid attack factor and the changes in the dimensions calculated for lower molarity(2M) to higher molarity(8M). If we see the NS/NH ratio as 1.5, it is clear that the higher is the attack factor, which results in a decrease in the mass and its dimensions from all four sides of the cube as compared to other ratios. Minimum AAF was observed for the NS/NH ratio of 2.5 due to the formation of the gel formations between them.



Fig: 2: AAF of Geopolymer Mortars 2,4,6,8M & NS/NH=1.5,2,2.5,3 for 7,14,28,56,90Days in Ambient(S) & Oven(O) in H_2SO_4

Acid Strength Loss Factor:

Fig:3 shows the acid strength loss factor, which can be defined as the variation of the change in the strength of the sample after immersion in the acid to the original strength of the sample before immersion in acid. It can write as

$$(ASLF)_{DAYS} = \frac{(\text{change in the strength of the sample after immersion in sulphuric acid})}{(\text{original strength of the sample before immersion in sulphuric acid})} \times 100$$

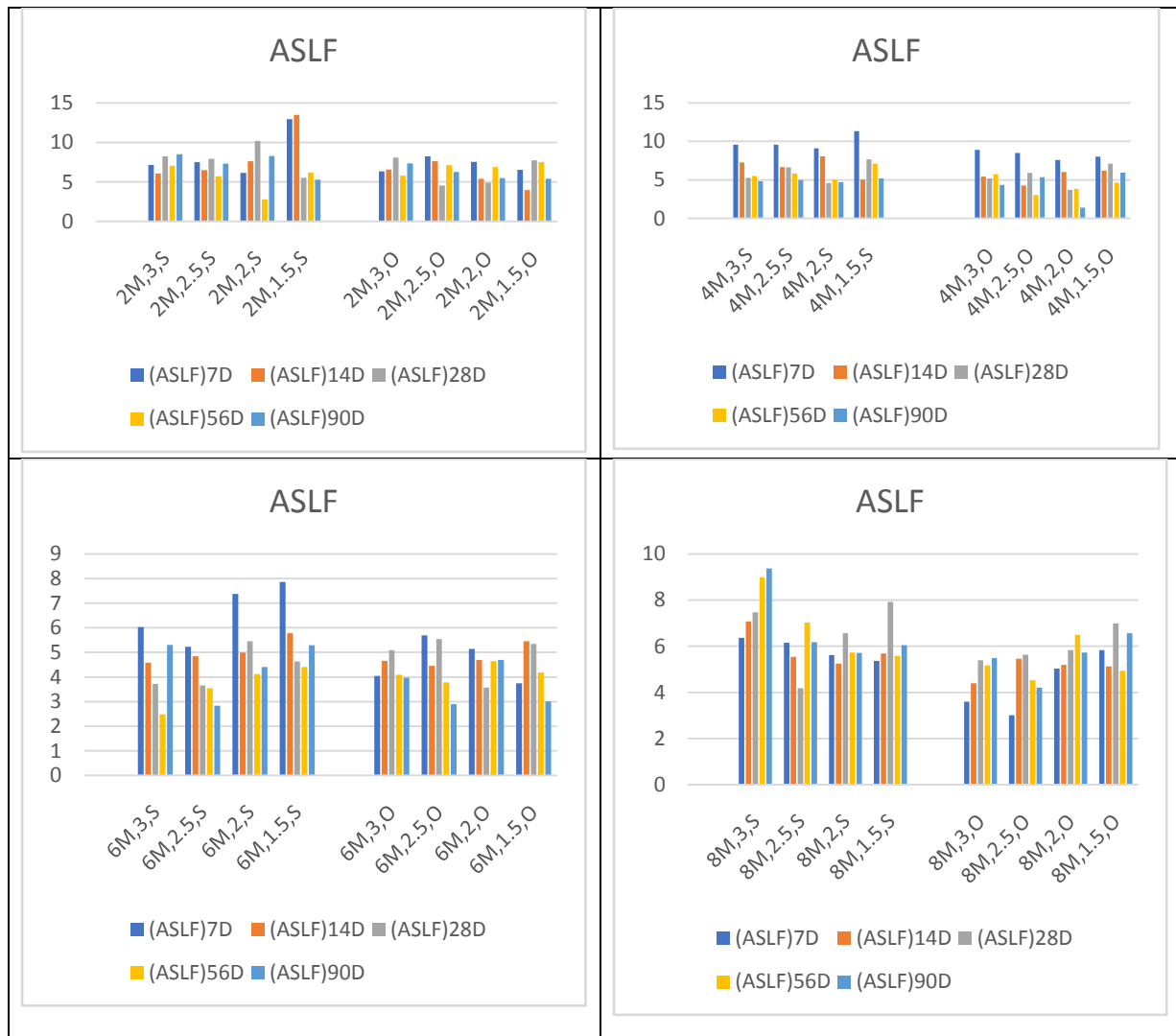


Fig: 3: ASLF of Geopolymer Mortars 2,4,6,8M & NS/NH=1.5,2,2.5,3 for 7,14,28,56,90Days in Ambient(S) & Oven(O) in H₂SO₄

Acid durability loss factor:

Fig:4 shows the Acid durability loss factor, and Acid durability loss factor defined as the loss that has taken place by the change in the mass, change in the dimensions and change in the strength of the sample constitutes the durability loss factor

It can write as

$$(ADFL)_{DAYS} = (AMLF) \times (AAF) \times (ASLF)$$



Fig: 4: ADLF of Geopolymer Mortars 2,4,6,8M & NS/NH=1.5,2,2.5,3 for 7,14,28,56,90Days in Ambient(S) & Oven(O) in H₂SO₄

SEM Analysis:

The morphology of the geopolymer mortar samples after 28 days of being heated to 60 degrees Celsius can be seen in this image captured by a scanning electron microscope. The differences in molarity and formation are depicted in the four images that have been presented thus far. If we take a look at the picture of the 2M, 1.5 Ratio of sodium silicate to sodium hydroxide, we can see that the production of voids and the irregular and shaky formation of polymerisation in the form of zeolites are both present. If we look at the 4M,1.5 SEM image, we can see that there is a presence of voids; nonetheless, fly ash particles react, and the formation is better than it is for 2M,1.5 ratios. The samples with a molarity of 6M and 8M exhibit active geopolymer gel formation in the form of sodium aluminium silicate and sodium silicate, respectively. There is clear evidence of the specimens in the dissolution of the fly ash particles, which indicates that gel is forming in the geopolymer mortar samples. The geopolymer mortar specimens exhibit stable polymerisation, as seen by the rod-like features in several of the samples. The SEM photos demonstrate how the early fractures have occurred in figure.5 & 6, respectively, of 2M, 2.5, and S ambient cured, which directly impacts the minerals generated in the XRD as well as the strength and Durability properties of the Geopolymeric samples. On the other hand, the oven-cured samples exhibit stable polymerisation gel formations, which leads to an increase in the strength and stable minerals that have been examined in XRD using PDXL software. The photos also show the emergence of

voids in the oven-cured specimens and cracks that occurred in the specimens that were ambiently cured for 2M and 4M, respectively. While the fly ash particles are no longer present, the 6M and 8M solutions, respectively, go through the process of gel formation.

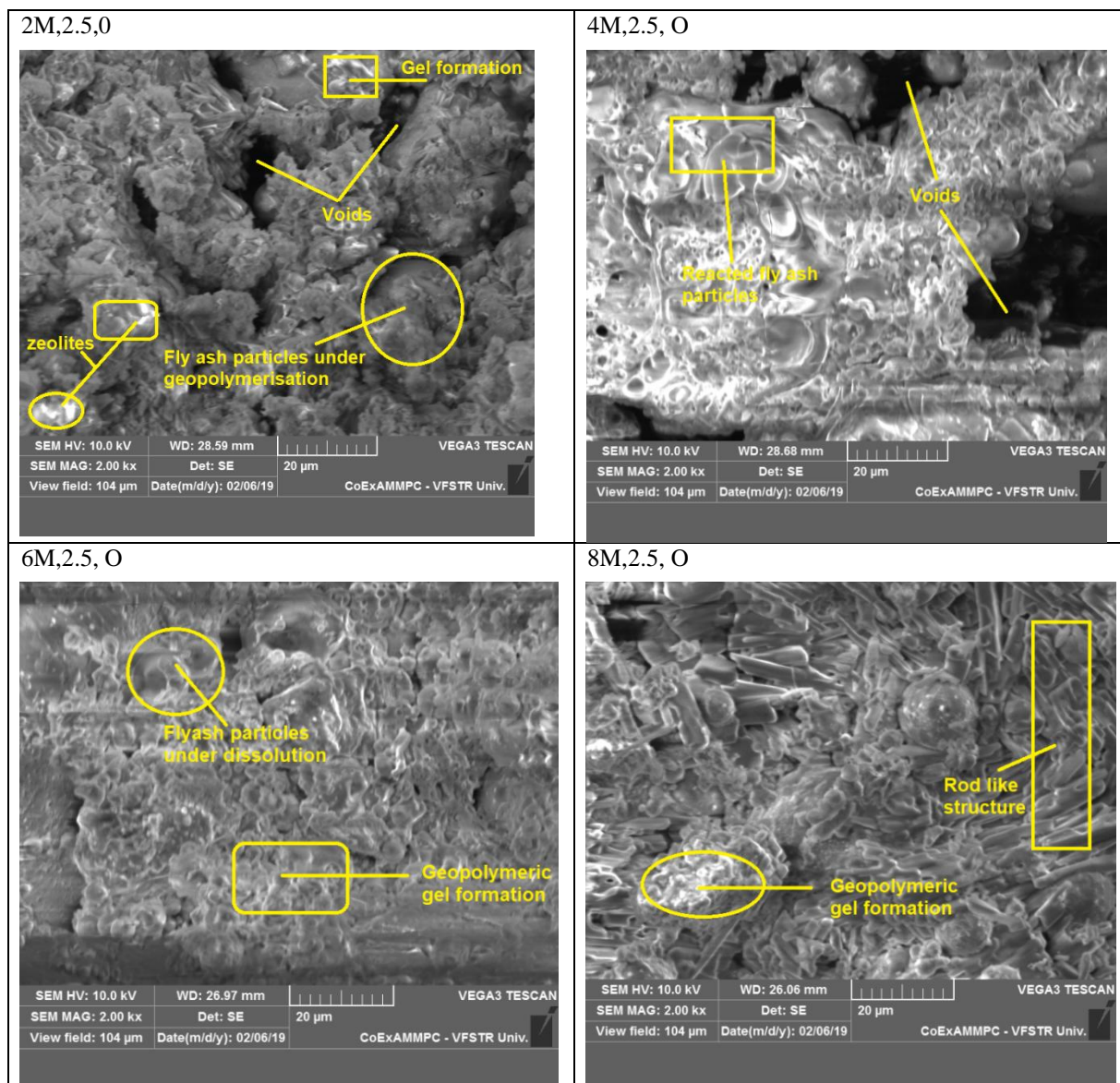


Fig: 5: SEM of Geopolymer Mortars 2,4,6,8M & NS/NH=2.5 for 28Days in Oven(O)

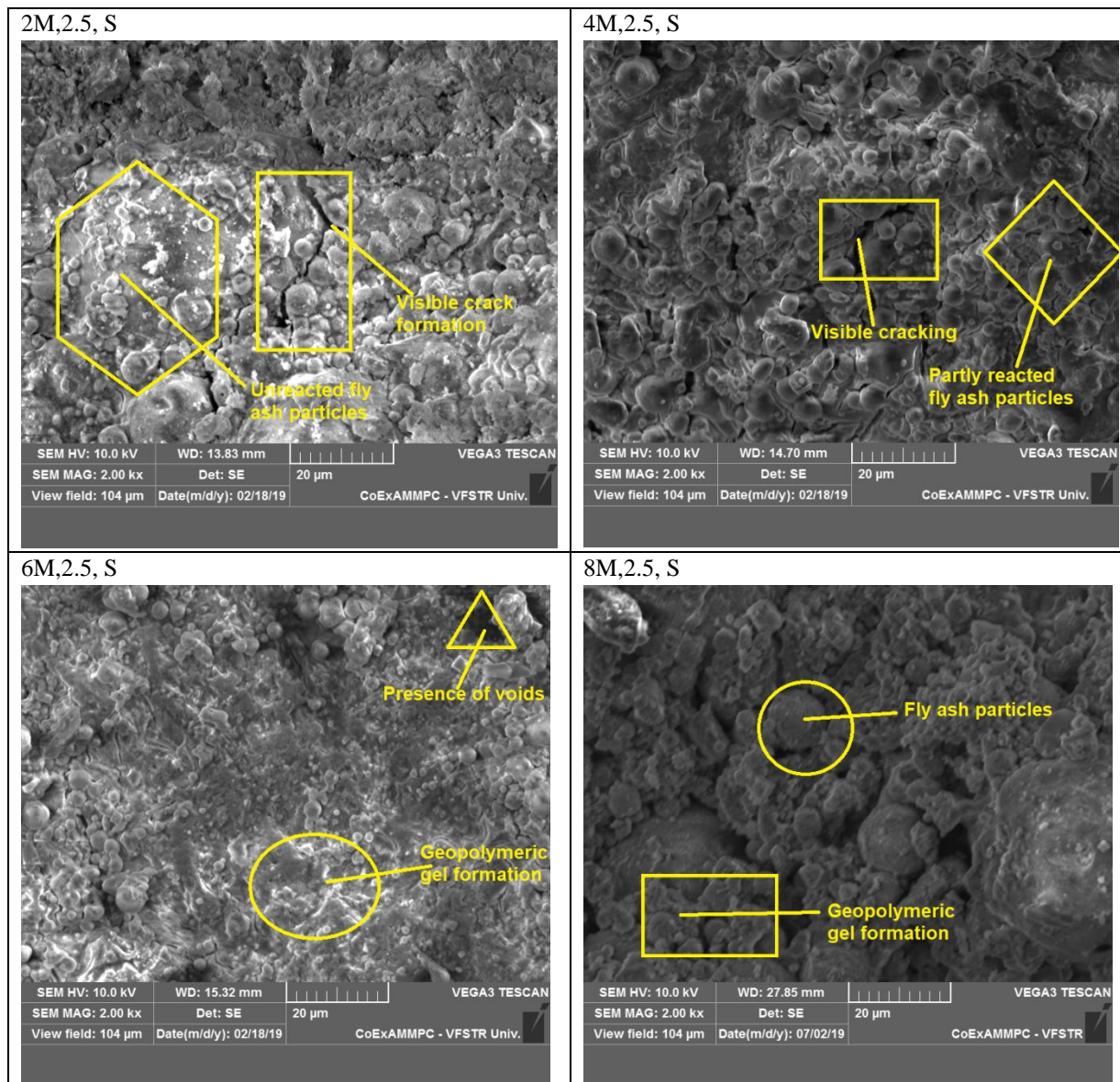


Fig: 6: SEM of Geopolymer Mortars 2,4,6,8M & NS/NH=2.5 for 28Days in Ambient(S)

XRD Analysis:

The mineral composition of the samples that were examined by the Xpert Hi-score plus programme can be seen by X-ray diffraction analysis. Crystalline peaks were found using XRD, showing that the mineral formation took the form of Quartz, Mullite, Hematite, Gismondine, Chabazite, Microcline, and sodium-calcium silicate. The authors report the same on the careful characterisation of the crystalline peaks that indicate the same minerals that have been found [5]. The geopolymer mortar specimens aged for 28 days have broad peaks detected at an angle of 25-30°C [8]. The minerals that were generated in this manner during the characterisation of the geopolymer mortar based on fly ash, as illustrated in figures 7 through 14. The Albite phase is formed due to the geopolymerization gel formation in geopolymer mortar. The formation of the albite phase is comparable to the formation of calcium sodium aluminium silicates [3], which has an effect on the development of strength in the geopolymer mortar specimens [5]. The complete quantification thus formed in examining X-ray diffraction minerals of both ambient and oven-cured specimens of 28 days is provided in table 1.

S.No:	Minerals Formed	Quantification in % Ambient				Quantification in % Oven			
		2M	4M	6M	8M	2M	4M	6M	8M
1	Quartz	51.5	46.5	27.7	28	51	40	35	34.3
2	Mullite	39.4	47.5	21.8	24	40	12	28	28.3
3	Hematite	4	-	3.9	-	4	-	-	-
4	Gismondine	5.1	-	-	-	4	-	-	3
5	Andradite	-	6.1	-	-	-	6	-	-
6	Microlite	-	-	32.7	30	-	-	-	-
7	Chabazite	-	-	4	-	-	-	-	-
8	Sodium calcium silicate	-	-	-	18	-	-	33	26.3
9	Albite	-	-	-	-	38	-	-	-
10	Rutile	-	-	-	-	1	4	-	-
11	Calcium Aluminium silicate	-	-	-	-	-	-	4	-
12	Calcium sodium aluminium oxide	-	-	-	-	-	-	-	8.1

Table: 1 XRD quantification of minerals

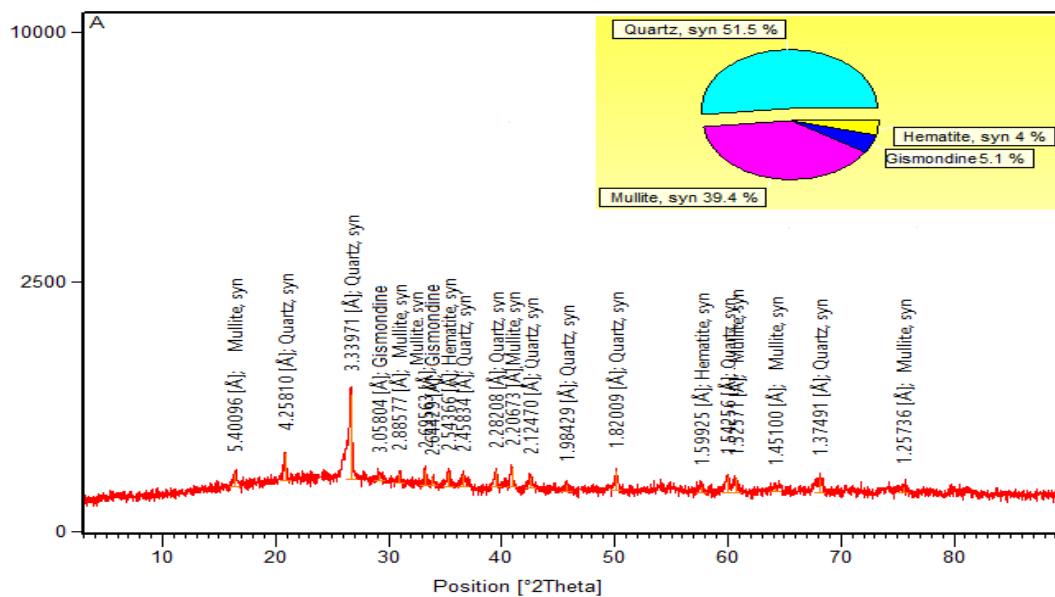


Fig: 7: XRD of Geopolymer Mortars 2M & NS/NH=2.5 for 28Days in Ambient(S)

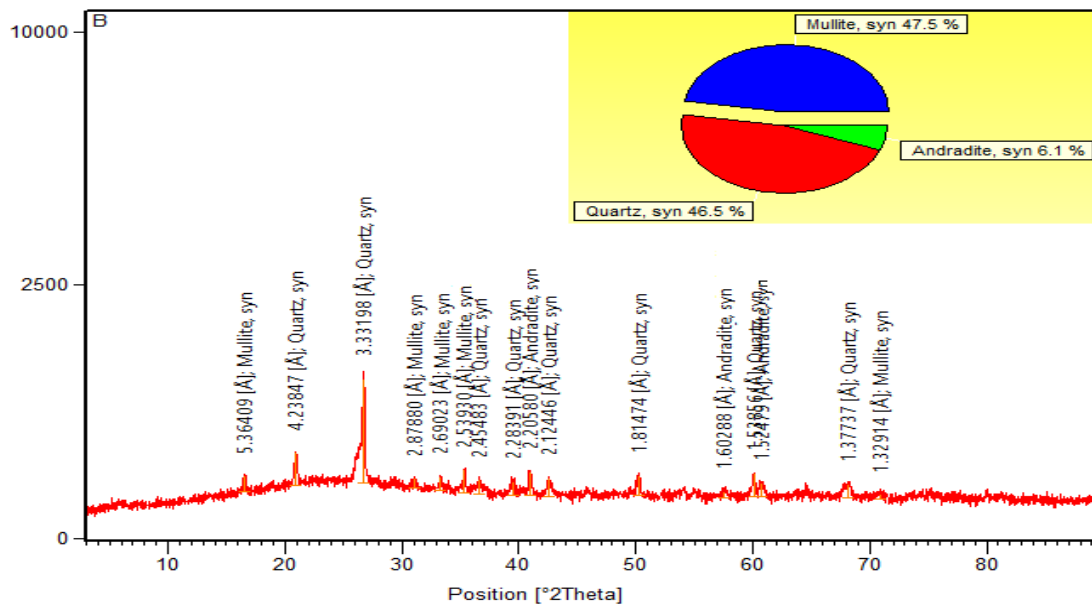


Fig: 8: XRD of Geopolymer Mortars 4M & NS/NH=2.5 for 28Days in Ambient(S)

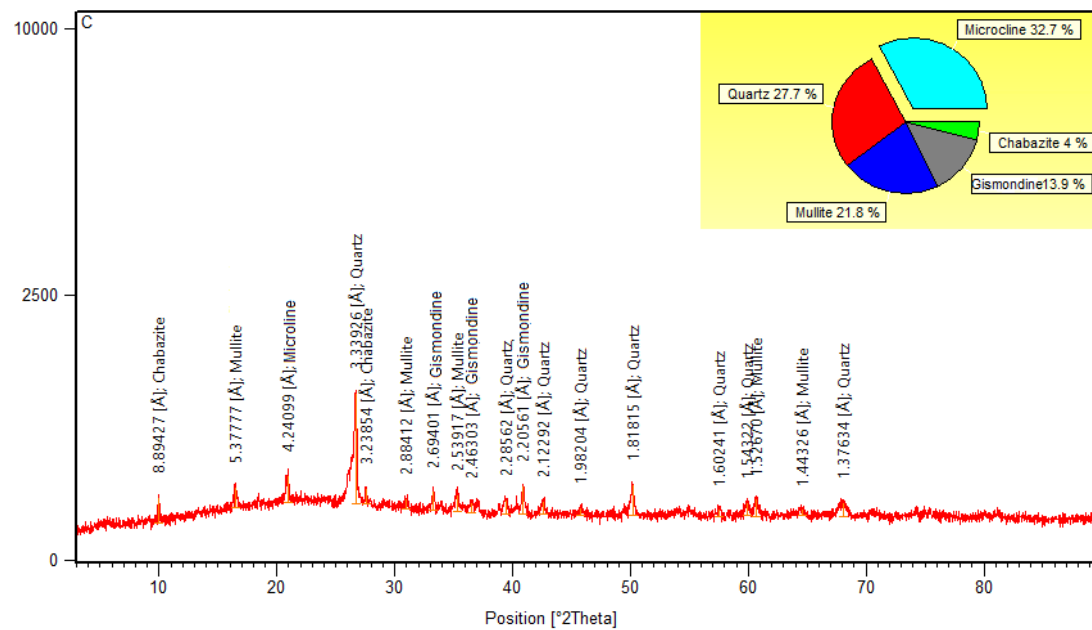


Fig: 9: XRD of Geopolymer Mortars 6M & NS/NH=2.5 for 28Days in Ambient(S)

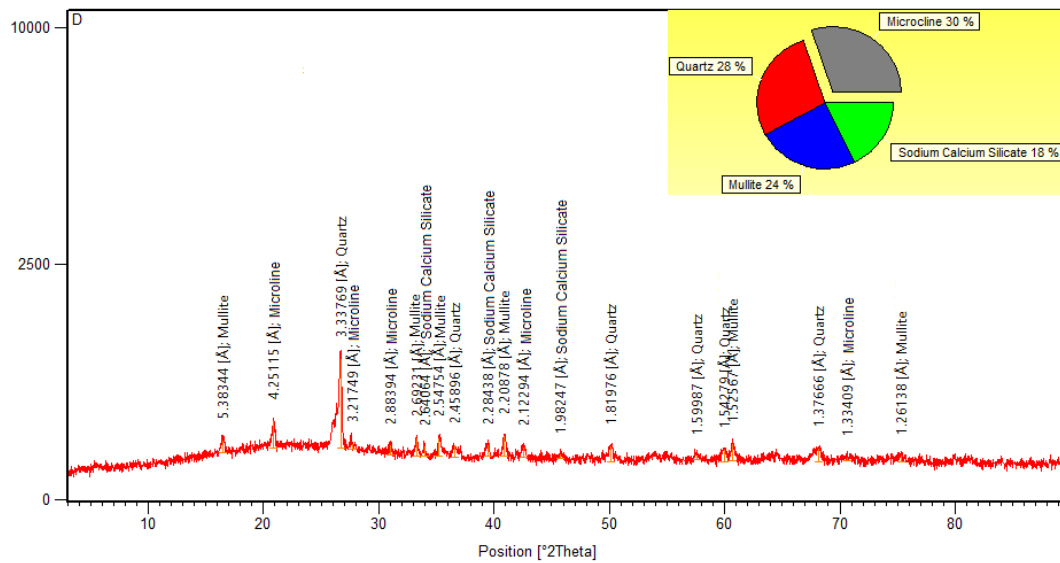


Fig: 10: XRD of Geopolymer Mortars 8M & NS/NH=2.5 for 28Days in Ambient(S)

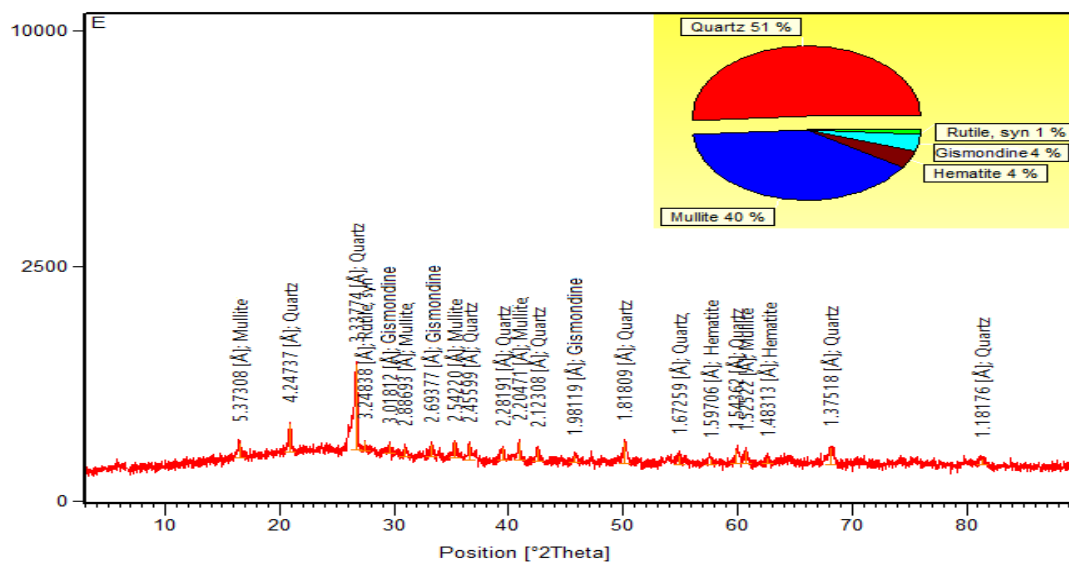


Fig: 11: XRD of Geopolymer Mortars 2M & NS/NH=2.5 for 28Days in Oven(O)

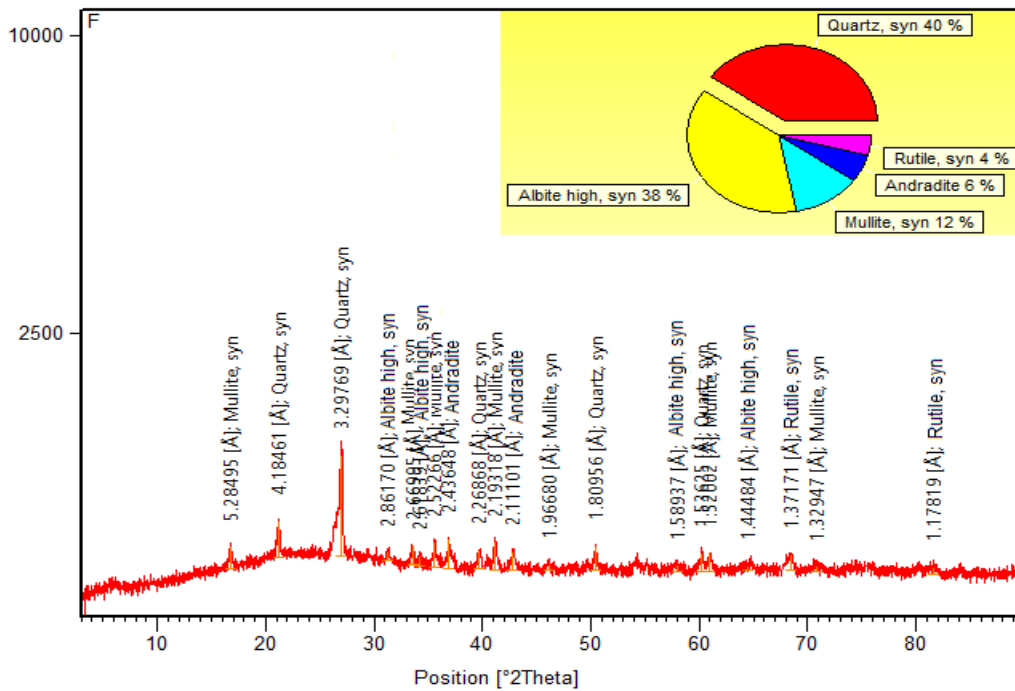


Fig: 12: XRD of Geopolymer Mortars 4M & NS/NH=2.5 for 28Days in Oven(O)

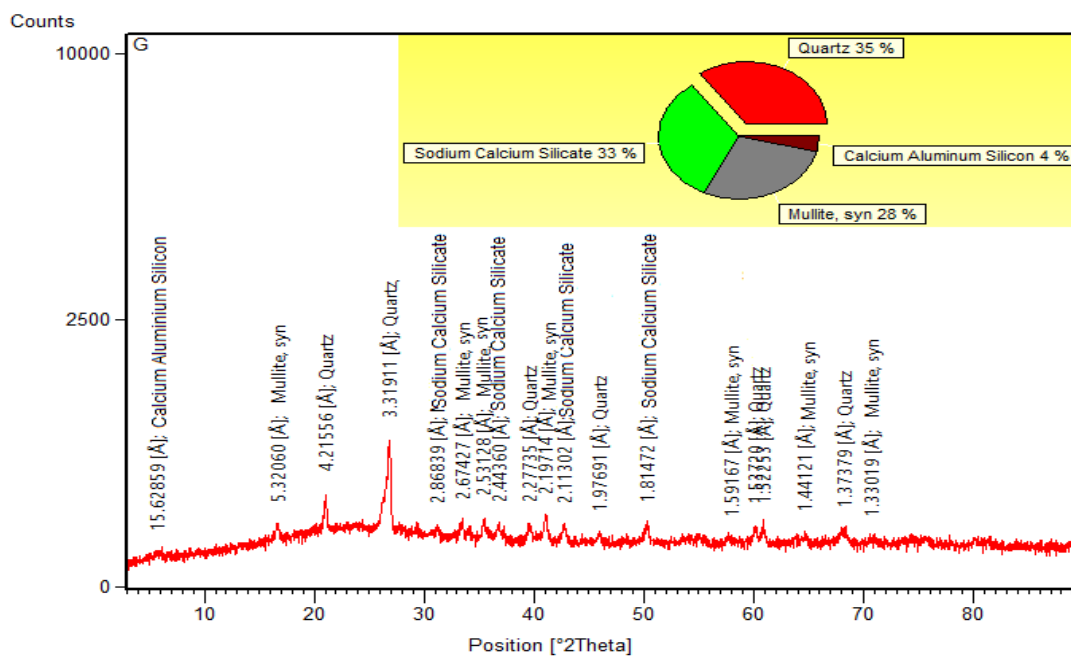


Fig: 13: XRD of Geopolymer Mortars 6M & NS/NH=2.5 for 28Days in Oven(O)

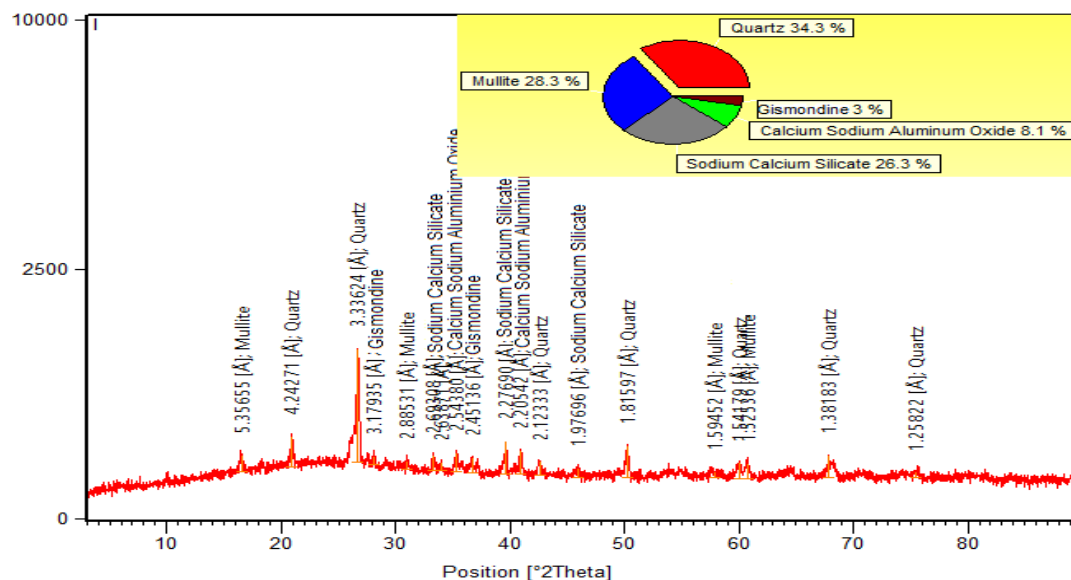


Fig: 14: XRD of Geopolymer Mortars 8M & NS/NH=2.5 for 28Days in Oven(O)

Conclusions:

SEM and EDS analysis reveals that fly ash consists of spherical particles that are abundant in aluminium and silicon. When the concentration of the sodium hydroxide solution is raised, the durability of all combinations of fly ash improves. On the other hand, the AMLF, AAF, ASLF, and ADLF values for sulphuric acid are lower when compared to those for nitric acid. A rise in NS/NH=1.5, 2 & 3 ratios has resulted in an increase in AMLF, AAF, ASLF, and ADLF; however, at NS/NH=2.5, it has obtained lower values of AMLF, AAF, ASLF, and ADLF for sulphuric acid in comparison to nitric acid. In the process of polymerisation and durability, the curing method plays a crucially important function. XRD and SEM photos have provided a clear explanation of the production of a strong geopolymer gel formation in the form of Na-Ca-Al-Si, which ultimately leads to an increase in the strength of geopolymer mortar.

Funding declaration:

No funding was received to carry out this study

ACKNOWLEDGEMENT:

The authors thank Vignan's Foundation for Science Technology & Research (Deemed to be University), Guntur, Andhra Pradesh, for the full support from the Center of Excellence for Advanced Materials, Manufacturing, Processing and Characterization (CoExAMMPC) for providing the Microstructure characterisations.

Author Contributions Statement:

1. Bohra Vinay Kumar Jain: Conceptualization, Methodology, Software, Data curation, Writing - original draft.
2. Nerella Ruben: Supervision, Conceptualization, Methodology, Software, Data curation, Writing - original draft.
3. Madduru Sri Rama Chand: Visualization, Investigation, Software, Validation, Writing - review & editing.

Conflict of interest:

The authors declare that they have no known competing financial interests or personal relationships that could have appeared to influence the work reported in this paper. There is no conflict of interest of work in this study.

REFERENCES

1. Keun-Hyeok Yang, Hey-Zoo Hwang, Seol Lee. "Effect of Water-Binder Ratio and Fine Aggregate - Total Aggregate ratio on the Properties of Hwangtoh- Based Alkali Activated Concrete", JOURNAL OF MATERIALS IN CIVIL ENGINEERING © ASCE vol. 22, no. 9, (2010), pp. 887-896.
2. Jian He, Guoping Zhang, P.E., M. ASCE, Shuang Hou, Cai CS. "Geopolymer-Based Smart Adhesives for Infrastructure Health Monitoring: Concept and Feasibility", JOURNAL OF MATERIALS IN CIVIL ENGINEERING © ASCE, vol. 23, no. 2, (2011), pp. 100-109.
3. Chindaprasirt, P., Chareerat, T., Hatanaka, S., Cao, T. "High-Strength Geopolymer Using Fine High-Calcium Fly Ash", JOURNAL OF MATERIALS IN CIVIL ENGINEERING © ASCE, vol. 23, no. 3, (2011), pp. 264-270.
4. Chaicharn Chotetanorm, Prinya Chindaprasirt, Vanchai Sata, Sumrerng Rukzon, Apha Sathonsaowaphak. "High-Calcium Bottom Ash Geopolymer: Sorptivity, Pore Size, and Resistance to Sodium Sulfate Attack", JOURNAL OF MATERIALS IN CIVIL ENGINEERING © ASCE, vol. 25, no. 1, (2013), pp. 105-111.
5. Kunal Kupwade-Patil, Erez, N., Allouche, P. Eng., "Examination of Chloride-Induced Corrosion in Reinforced Geopolymer Concretes", JOURNAL OF MATERIALS IN CIVIL ENGINEERING © ASCE, vol. 25, no. 10, (2013), pp. 1465-1476.
6. Reddy, D.V., ASCE PE, M., Jean-Baptiste Edouard, Khaled Sobhan, A.M. ASCE. "Durability of Fly Ash-Based Geopolymer Structural Concrete in the Marine Environment", JOURNAL OF MATERIALS IN CIVIL ENGINEERING © ASCE, vol. 25, no. 6, (2013), pp. 781-787.
7. Dali Bondar. "Use of a Neural Network to Predict Strength and Optimum Compositions of Natural Alumina-Silica-Based Geopolymers", JOURNAL OF MATERIALS IN CIVIL ENGINEERING © ASCE, vol. 26, no. 3, (2014), pp. 499-503.
8. Sudhakar M. Rao, "Indra Prasad Acharya. Synthesis and Characterization of Fly Ash Geopolymer Sand", JOURNAL OF MATERIALS IN CIVIL ENGINEERING © ASCE, vol. 26, no. 5, (2014), pp. 912-917.
9. Muhammad Aamer Rafique Bhutta, Warid M. Hussin, Mohd Azreen, Mahmood Mohd Tahir. "Sulphate Resistance of Geopolymer Concrete Prepared from Blended Waste Fuel Ash. Journal of Materials in Civil Engineering", © ASCE, vol. 26, no. 11, (2014), pp. 04014080-1-6.

10. Gingham Maranan, Allan Manalo, Karu Karunasena, Brahim Benmokrane. "Bond Stress-Slip Behavior: Case of GFRP Bars in Geopolymer Concrete", *Journal of Materials in Civil Engineering*, vol. 27, no. 1, (2015), pp. 04014116-1-9.
11. Patimapon Sukmak, Pre De Silva, Suksun Horpibulsuk, Prinya Chindaprasirt, P.E. "Sulfate Resistance of Clay-Portland Cement and Clay High-Calcium Fly Ash Geopolymer", *Journal of Materials in Civil Engineering*, © ASCE, vol. 27, no. 5, (2015), pp. 04014158-1-11.
12. Ali Nazari, Jay G. Sanjayan. "Modeling of Compressive Strength of Geopolymers by a Hybrid ANFIS-ICA Approach", *Journal of Materials in Civil Engineering*, © ASCE, vol. 27, no. 5, (2015), pp. 04014167-1-8.
13. Erdogan, S.T. "Properties of Ground Perlite Geopolymer Mortars", *Journal of Materials in Civil Engineering*, © ASCE, vol. 27, no. 7, (2015), pp. 04014210-1-10.
14. Arul Arulrajah, Teck-Ang Kua, Chayakrit Phetchuay, Suksun Horpibulsuk, Farshid Mahghoolpilehrood, Mahdi Miri Disfani. "Spent Coffee Grounds-Fly Ash Geopolymer Used as an Embankment Structural Fill Material", *Journal of Materials in Civil Engineering*, © ASCE, vol. 28, no. 5, (2016), pp. 04015197-1-8.
15. Itthikorn Phummiphan, Suksun Horpibulsuk, Tanakorn Phoo-ngernkham PE, Arul Arulrajah, Shui-Long Shen. "Marginal Lateritic Soil Stabilized with Calcium Carbide Residue and Fly Ash Geopolymers as a Sustainable Pavement Base Material", *Journal of Materials in Civil Engineering*, © ASCE, vol. 29, no. 2, (2017), pp. 04016195-1-10.
16. Albitar, M., Visintin, P., Mohamed Ali, M.S., Lavigne, O., Gamboa, E. "Bond Slip Models for Uncorroded and Corroded Steel Reinforcement in Class-F Fly Ash Geopolymer Concrete", *Journal of Materials in Civil Engineering*, © ASCE, vol. 29, no. 1, (2017), pp. 04016186-1-10.
17. Yan-Jun Du, Bo-Wei Yu, Kai Liu, Ning-Jun Jiang, S.M. ASCE, Martin D. Liu. "Physical, Hydraulic, and Mechanical Properties of Clayey Soil Stabilized by Lightweight Alkali-Activated Slag Geopolymer. *Journal of Materials in Civil Engineering*", © ASCE, vol. 29, no. 2, (2017), pp. 04016217-1-10.
18. Indian Standards: 383-1970, Specification for coarse and fine aggregates from natural sources for concrete, Bureau of Indian Standards, New Delhi, India.
19. Indian Standards: 516-1956 (Reaffirmed 1999), Indian Standard Methods of Tests for Strength of Concrete, Bureau of Indian Standards, New Delhi, India.
20. ASTM C 666-97, Standard Test Method for Resistance of Concrete to Rapid Freezing and Thawing, ASTM International, West Conshohocken, PA, USA.